AN ALTERNATIVE IMAGE PROCESSING APPROACH FOR THE VIABILITY OF CELLS BY LIGHT MICROSCOPY

A MASTER'S THESIS

in

Electrical & Electronics Engineering

Atilim University

by

AKIN ÖZKAN

JULY 2011

AN ALTERNATIVE IMAGE PROCESSING APPROACH FOR THE VIABILITY OF CELLS BY LIGHT MICROSCOPY

A THESIS SUBMITTED TO

THE GRADUATE SCHOOL OF NATURAL AND APPLIED SCIENCES

OF

ATILIM UNIVERSITY

BY

AKIN ÖZKAN

IN PARTIAL FULFILLMENT OF THE REQUIREMENTS FOR THE DEGREE OF

MASTER OF SCIENCE

IN

THE DEPARTMENT OF ELECTRICAL & ELECTRONICS

ENGINEERING

JULY 2011

Approval of the Graduate School of Natural and Applied Sciences,Atılım University.

_____

Prof. Dr. K. İbrahim Akman

Director

I certify that this thesis satisfies all the requirements as a thesis for the degree of Master of Science.

_____

Assoc. Prof. Dr. Elif Aydın

Head of Department

This is to certify that we have read the thesis "An Alternative Image Processing Approach for The Viability of Cells by Light Microscopy" submitted by "Akın Özkan" and that in our opinion it is fully adequate, in scope and quality, as a thesis for the degree of Master of Science.

_____	_____
Asst. Prof. Dr. S. Belgin İşgör	Asst. Prof. Dr. Hakan Tora
Co-Supervisor	Supervisor

Examining Committee Members

Asst. Prof. Dr. S. Belgin İşgör	_____
Asst. Prof. Dr. Hakan Tora	_____
Asst. Prof. Dr. Nergiz E. Çağıltay	_____
Prof. Dr. Özlem Yıldırım	_____
Assoc. Prof. Dr. Ziya Telatar	_____

Date: July 20, 2011

I declare and guarantee that all data, knowledge and information in this document has been obtained, processed and presented in accordance with academic rules and ethical conduct. Based on these rules and conduct, I have fully cited and referenced all material and results that are not original to this work.

Name, Last name: AKIN ÖZKAN
Signature:

ABSTRACT

AN ALTERNATIVE IMAGE PROCESSING APPROACH FOR THE VIABILITY OF CELLS BY LIGHT MICROSCOPY

Özkan, Akın

M.S., Electrical & Electronics Engineering Department

Supervisor: Asst. Prof. Dr. Hakan Tora

Co-Supervisor: Asst. Prof. Dr. S. Belgin İşgör

July 2011, 55 pages

The methods to determine the amount and viability of cells play an important role in the field of microbiology and cell biology. The basic cell counting process is through microscopic analysis using hemocytometer, performed by a technician. In this process, the most economical and widely used technique is dye-exclusion method to determine cell number and viability. In this study, a novel image based approach for cell counting (NIBA-C) is proposed with a capability of distinction between alive from death during the process. For evaluating the success of proposed method, the results obtained by the method are compared with microscopic cell viability count by virtue of classical dye-exclusion method. The method depends first on segmentation of the cells and then classification of them. Segmentation of cell images is achieved using Hough Transform. Artificial Neural Network is used to distinguish cell images from non-cells and death cell images from alive cells.

In this study, it is concluded that the cell analysis by NIBA-C accomplishes 70 % more accuracy in finding the correct location of the cells, and more than 50% reliable in defining viable cells in comparison with the classical cell count method based on dye-exclusion.

Keywords: HL-60 Cell Counting, Hough Transform, Artificial Neural Network

ÖZ

IŞIK MİKROSKOBU KULLANARAK HÜCRE SAYIMI İÇİN ALTERNATİF BİR GÖRÜNTÜ İŞLEME YAKLAŞIMI

Özkan, Akın

Yüksek Lisans, Elektrik - Elektronik Mühendisliği Bölümü

Tez Yöneticisi: Yrd. Doç. Dr. Hakan Tora

Ortak Tez Yöneticisi: Yrd. Doç. Dr. S. Belgin İşgör

Temmuz 2011, 55 sayfa

Hücre sayımı ve bu hücrelerin sınıflandırılması için kullanılan yöntemler mikro biyoloji ve hücre biyolojisi alanında önemli bir yer tutmaktadır. En temel sayma mikroskop aracılığıyla Hemositometre kullanılarak insan tarafından yapılır. Bu süreçte hücre sayısı ve canlılığını belirlemek için kullanılan en ekonomik ve en yaygın teknik boya dışlama yöntemidir. Bu çalışmada, hücre canlı-ölü ayrımı yapabilen yeni bir görüntü tabanlı hücre sayımı yaklaşımı(NIBA-C) önerilmiştir. Önerilen yöntemin başarısını değerlendirmek için aynı görüntüler, yöntem ile elde edilen değerler klasik boya dışlama yöntemi ile elde edilen sonuçlar ile karşılaştırılmıştır. Yöntemi segmentasyon ve ardından görüntülerin sınıflandırılması oluşturur. Segmentasyon aşamasında Hough Dönüşümü kullanılmıştır. Yapay Sinir Ağları hücre-hücre olmayan ve canlı-ölü hücre görüntü sınıflandırmasında kullanılmıştır.

Bu çalışmada; önerilen yöntem NIBA-C %70 in üzerinde yerbulma ve %50 üzerinde canlı ölü ayrımı yapabilme yetenegi sergilemiştir.

Anahtar Kelimeler: HL-60 Hücre Sayımı, Hough Dönüşümü, Yapay Sinir Ağı

To My Family

ACKNOWLEDGMENTS

I would like to express my gratitude to my dear advisors Asst. Prof. Dr. Hakan Tora and Asst. Prof. Dr. S. Belgin İşgör for their valuable support, guidance, insight, patience, and encouragement throughout the study. This research could have never been possible without their support.

I wish to express my thanks to Asst. Prof. Dr. Nergiz E. Çağıltay, Prof. Dr. Özlem Yıldırım and Assoc. Prof. Dr. Ziya Telatar for their valuable suggestions and corrections.

Many people have supported my work directly or indirectly. Among them my family, who supported and encouraged me while doing my thesis. I would like to express my thanks to Dr. Yasemin İşgör and Dr. Pembegül Uyar for the help given during the various stages of my thesis. And last but not the least I would like to thank Atilim University Electrical and Electronic academic staff and my colleagues for their sympathy.

This research is financially supported by Republic of Turkey, Prime Ministry, State Planning Organization (DPT) under "İmge İşleme Tabanlı Otomatik Hücre Analiz Sistemi-Toma Kullanılarak Boya Dışlama Esaslı Hücre Sayımı, Canlılık Sayımı ve Hücre Morfolojisi Analizi", ATÜ P2006 06 project.

TABLE OF CONTENTS

LIST OF TABLES

LIST OF FIGURES

LIST OF ABBREVIATIONS

HT	-	Hough Transform
CHT	-	Circular Hough Transform
HL-60	-	Human Promyeloblastic Leukemia
TB	-	Trypan Blue
ANN	-	Artificial Neural Network
RBC	-	Red Blood Cell
WBC	-	White Blood Cell
RGB	-	Red Green Blue

CHAPTER 1

INTRODUCTION

The term of image processing refers to two primary objectives; first, improvement of image quality for human visual. Second, processing input image to reach meaningful output data for machine perception [1]. Number of image processing applications increase each day due to computing power of computers. Today, the most known image processing applications are face detection [2], license plate recognition [3], and satellite image improvement [4]. Nowadays, there are frequent applications of the image processing techniques in the field of cell biology.

Microscopic cell counting has been used in biology, medicine, and chemistry. The counting of cells provides invaluable information for diagnosis and treatment of many diseases. Also this process may give information about cell culture's condition to examiner. Dead cells are increasing when their environment is unsuitable to live or if some chemicals added all these additional materials negatively effect cell culture conditions.

In ordinary cell culture studies, the cells are counted manually by the researchers using hemocytometer under microscope. The hemocytometer has ruled area consists of several, large, 1 x 1 mm (1 mm^2) squares each has defined volume. The images under microscope first magnified with 10x and then 40x magnifications are set to count the cells.

The counting process is completed by scanning the area on the hemocytometer under microscope. During the manual counting process from sample to sample the main problem is time consuming task and also its accuracy changes with experience of the examiners, the tiredness of examiner is another problem.

As a result of this, automated cell counting system is very helpful to improve accuracy of counting and accelerate the counting procedure. There are also few commercial automatic cell counting systems available. But the costs of these systems are too high to be used commonly.

1.1. Scope of the Thesis

Our aim in this study is to develop image processing based, automated cell viability count technique using Hemocytometer cell counting method. Cell viability covers all the decision making process of dead or alive cells. But for automation of cell counting top to bottom; first, cell positions have to be known and using this location information they must be separated from input image. For this reason this study is divided into two parts. First part is organized to find the location of cells on the given image. Second part is established for distinction of dead cells from the alive ones by using cropped images after finding the position of cells data.

The study is initiated with the images analyzed under 40x magnified objective of microscopy and then extended with investigation under 10x. Figure 1 shows the difference between 10x and 40x magnified image samples under microscope.

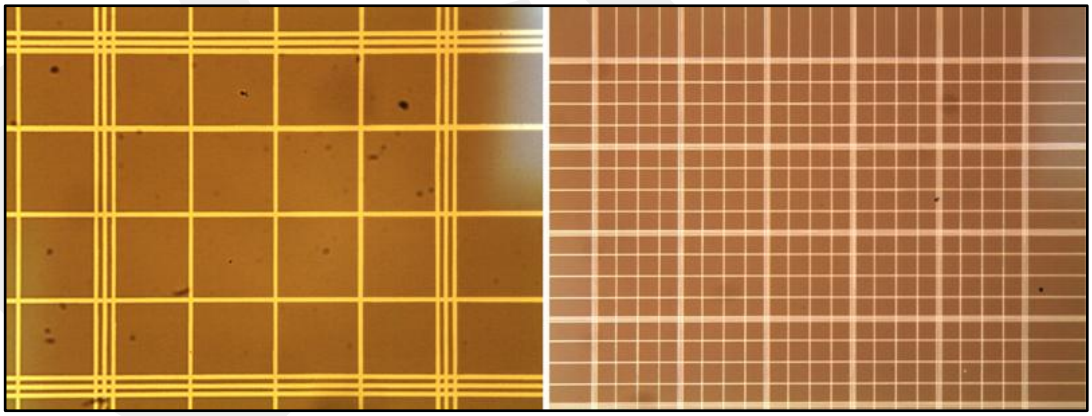

Figure 1. The images of the cells (dark spots) on hemocytometer under 40x (left) and 10x magnified objective (right) of microscope.

In this study, two solutions which are slightly different from each other, depending on the magnification settings such as 10x and 40x of the microscope, are proposed.

Two paths can be followed for each setting. The first path is the use of Kuwahara Filter [5]. Second path uses circular averaging filter as the first path does. The only difference between these two paths is the use of filter in different kernel sizes. All these paths are summarized on Figure 2 and Figure 3 respectively.

In the first step of 40x magnified input images are filtered by using circular averaging filter which has a kernel size of 3. The raw input image and the image filtered through circular averaging filter are segmented by following the steps of Edge detection [6] and Hough Transform [7]. The segmented images are then classified as ‘cell’ or ‘non-cell’ and ‘alive’ or ‘death’ and finally the images are counted.

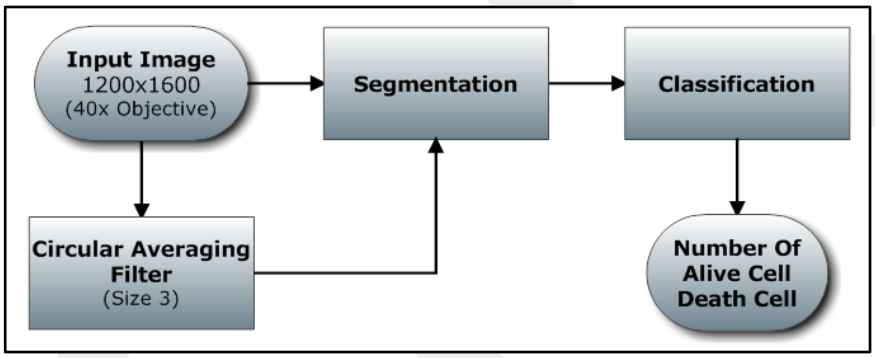

Figure 2. Block Diagram of the first step of 40x magnified input images.

The second path follows 10x magnified images first filtered with the different circular averaging filter having different kernel sizes of 1, 2, and 3. Each image from this step is segmented individually. Then the images are classified and counted too.

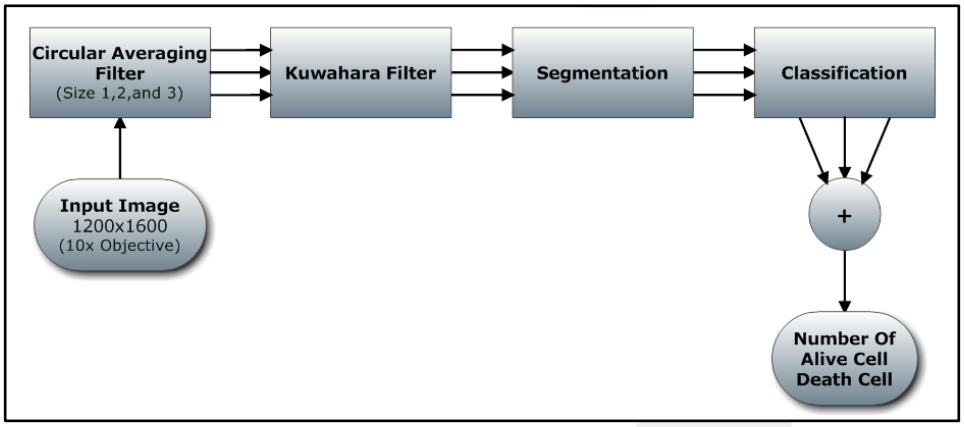

Figure 3. Diagram of the first step of 10x magnified input images

1.2. Organization of the Thesis

The thesis is organized as follows. Chapter 2 presents a literature survey on cell counting and Hemocytometer based cell counting. Chapter 3 is an overview of the image edge detection, Hough transform and their applications. The classification of images is listed in Chapter 4. In Chapter 5 the results are presented and all discussions and conclusions about the study are listed in Chapter 6.

1.3. Equipments in use

During the cell count process there are two fundamental equipments. First one is the light microscopy and second one is the "counting chambers" included Hemocytometer. Additionally, a computer connected CCD camera which is also attached to the microscope is used to take the images under microscopy. The chemical, Trypan blue (TB) stain is used to distinguish live cells from the deaths.

1.3.1. Light Microscopy

The capacity of observing cells has always been dependent on the level of convenient technology [8]. Modern light microscope consists of some essential parts [9].

Fundamental parts of the microscope are shown in Figure 4;

1. Eyepiece
2. Objective turret (it holds multiple objective lenses)
3. Frame
4. Focus wheel to move the stage (coarse and fine adjustment)
5. Light source

Figure 4. Light Microscopy essential parts

1.3.2. CCD Camera

The public available HL-60 cell image database has not been encountered up to date. Therefore a data set is prepared for this study by the captured images. Images have taken by 2.0 Megapixels Moticam 2000 CCD camera (1200x1600 pixels) from Motic B3-Series model microscope. The HL-60 dataset used in this study consists of 220 images obtained from 10x magnification and 900 images from 40x. These dataset are also used for training the Artificial Neural Network, ANN.

1.3.3. Hemocytometer

The most widely used cell counting technique is called Hemocytometer counting. Hemocytometer is a piece of glass on which the lines are drawn to a certain size to help manual counting (counting chamber).

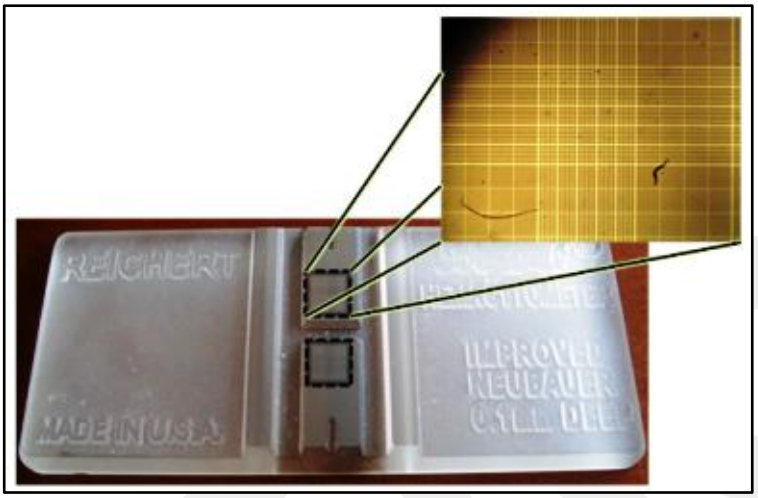

Figure 5. Hemocytometer and Counting chamber

It contains particular volume of solution. Using count of cell sample, cells/ml can be calculated for getting information about over all cell suspension (Figure 5). Each square of the hemocytometer (with cover slip in place) represents a total volume of 0.1 mm^3 or 10^{-4} cm^3. Since 1 cm^3 is equivalent to 1 ml, the subsequent cell concentration per ml (and the total number of cells) will be determined using the following equations:

Cells/ml = the average count per square × the dilution factor×10^4.

Total cell number = cells/ml × the original volume of cell suspension from which cell sample was removed.

1.3.4. Trypan Blue

Trypan Blue is a stain used to separate dead and alive cells. Trypan Blue stain cannot enter inside the live cells but dead cells let the stain go inside. As a result of this, living cells appear brighter and dead cells look much darker during counting [10].

1.4. Manual HL-60 Counting Using Hemocytometer

The manual cell count using hemocytometer method has few steps. Counting protocol is as follows [11];

1. The counting chamber surface of hemocytometer and coverslip is cleaned by using ethanol.
2. The coverslip is placed over the counting chamber of hemocytometer.
3. The cell suspension (HL-60) is diluted by using TB solution.
4. The mixture of HL-60 and Trypan Blue solution is spread onto the counting chamber of hemocytometer.
5. 40x magnification of microscope is set for counting.
6. Cell counts are recorded for each of the central squares on hemocytometer.
7. The number of cells per milliliter is determined and the single manual cell counting process is accomplished

If a new set of cell count is necessary then all steps are repeated.

CHAPTER 2

LITARETURE SURVEY ABOUT CELL COUNTING

Although there have been many studies in the literature related to automated cell counting, only a few of them are related with the automated hemocytometer cell counting.

2.1. Automated Cell Counting

The cell culture field has a lot of different types of cells and each cell type has wide variety of shapes. There are some studies in which segmentation or counting methods for different types of cells like nerve cell [12], white blood cell [13], or malaria cell [14] are discussed.

In the literature there are two groups of studies related with cell segmentation and cell counting. In those studies cell segmentation method is just used to find the location of cells as perfect as possible [15,16]. In those studies the segmentation step is not used to determine the number of cells. In the other studies in which cell counting technique is primarily discussed, the segmentation is used just as a step for the counting process [17, 18]. Mathematical morphology techniques are also discussed in the literature for cell segmentation [19, 20].

In some studies machine learning algorithms are also adapted to find the location of cells [21, 22]. In those studies, segmentation step is skipped and the input images are cropped manually by the investigators and then the cropped images are classified by machine learning algorithms [23, 24, 25].

Additionally, in some studies hybrid methods are proposed. For example, Fabio S. combined the morphological analysis and ANN [26]. Savkare and Narote used support vector machine, SVM in which images are classified after the use of watershed transform [27]. Allan et al. performed unsupervised cell segmentation [28].

2.2. Automated Hemocytometer Based Cell Counting

Automated hemocytometer cell counting method is used to obtain accurate information about the concentration of cells in overall suspension [29]. In the study performed by the Brinda et al. using leukemia cells; cells are segmented using recursive algorithm and in the later study of this group the application of the segmentation method the statistical analysis of leukemia cell population is given. In these studies, hemocytometer and image processing techniques are used including with median filter and Prewitt gradient map [30, 31].

In another study, Nasution and Suryaningtyas compared red blood cell counting algorithm which is based on the connected component labeling and ANN [32]. In that study, the images of only which the cells are focused (over focusing) are taken to eliminate the background effect. Besides, the watershed segmentation algorithm is utilized too to get a clearer boundaries among clumped cells (cells attached each other).

Claudio and Leonilda established a study which is based on the blood samples of three wild animals Nasua nasua; Brazilian aardvark, Leopardus pardalis; dwarf leopard, and a monkey Cebus paella. In this study, red blood cells are counted by using the captured images at two different focal settings [33]. In one study new software called Lohitha is introduced by G.P.M Priyankara et al. [34]. In that work it is proposed that the program is capable of counting various cell types efficiently.

In the literature there have been no study found to include solution for all adverse image conditions such as, cell shape deformation, different lightning conditions and brightness differences of images.

CHAPTER 3

SEGMENTATION OF HL-60 CELLS

Segmentation in image processing refers to extraction process of objects in a given image. There are a number of segmentation techniques [35] including pixel based, edge based, region based, and model based.

Pixel based image segmentation techniques are the simplest and fastest methods. Most pixel based segmentation procedures use thresholds in the histogram of image. Optimum threshold is determined by simple or complex algorithms.

Edge based segmentation commonly indicates the segmentation method that is based on the edge of image. Most of the time simple preprocessing methods are applied before the edge detection methods and then segmentation starts.

Region based methods have basic idea that the neighboring pixels within one region have similar values. The procedure is to check one pixel with its neighbors. If a similarity condition is satisfied, the pixel is assigned to the same group that includes its neighbors.

Model based segmentation is the construction of formation from the model of the existing structure. This form can be a simple geometrical model (e.g. line, circle) or a statistical model of the object. HL-60 cells have roughly circular shapes. Sometimes they may have shape deformation depending on the cell culture. The main difficulty is that while counting cells may come across onto white lines which are existed in Hemocytometer. Figure 6 illustrates some of these possibilities.

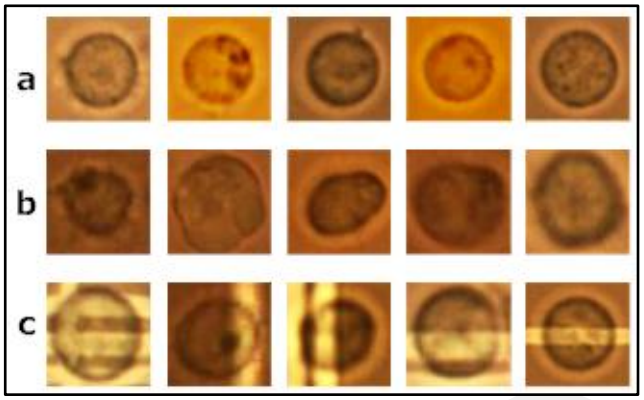

Figure 6. Circular cells (a), shape deformed cells (b), cells on white lines (c)

3.1. Image Filtering

Image filtering is a general operation of the enhancement of image quality from the given image using some algorithms. There are various types of different image filters utilized depending on the application at hand such as smoothing, sharpening, edge detection, etc. Filtering of an image can be performed either in frequency domain or in spatial domain [36]. Frequency domain techniques are based on Fourier transform of an image [1]. In contrast, spatial domain approaches are based on manipulating of pixels directly in an image.

3.1.1. Circular Averaging Filter

The term circular implies the shape of the filter window. Window size is obtained as followed:

$$2 \text{ x radius} + 1 \quad (1)$$

where radius is an integer number and chosen by user.

Figure 7 shows some of the kernels having different sizes. As the size of kernel is increased, the filtered image is getting smoother.

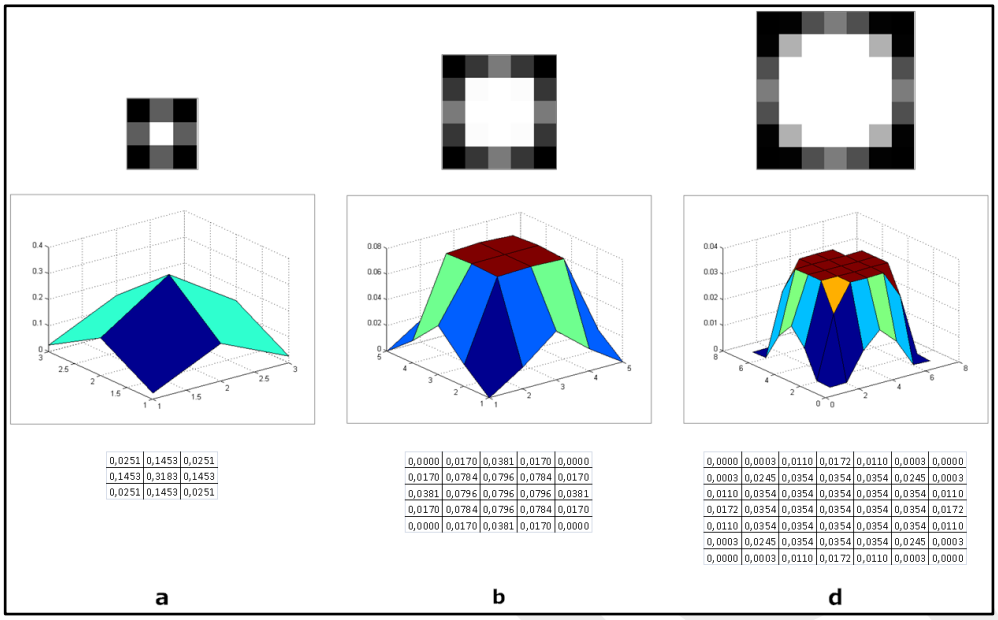

Figure 7. Circular Kernels for radius=1 (a), radius=2 (b), and radius=3 (c)

The main goals for the use of this filter are listed as follows [33]:

- Remove noise from image
- Emphasize circular shapes on image
- Obtain different focal settings using one image

3.1.2. Kuwahara Filter

After averaging filter, images are filtered by Kuwahara filter. Kuwahara filter is an edge preserving smoothing filter [5]. In other words, while the current image is getting smoother edges are preserved (Figure 8). We applied Kuwahara filter only to 10x objective images. When used on 40x magnified objective images Kuwahara filter causes much longer processing time and decreases accuracy of finding the cell location.

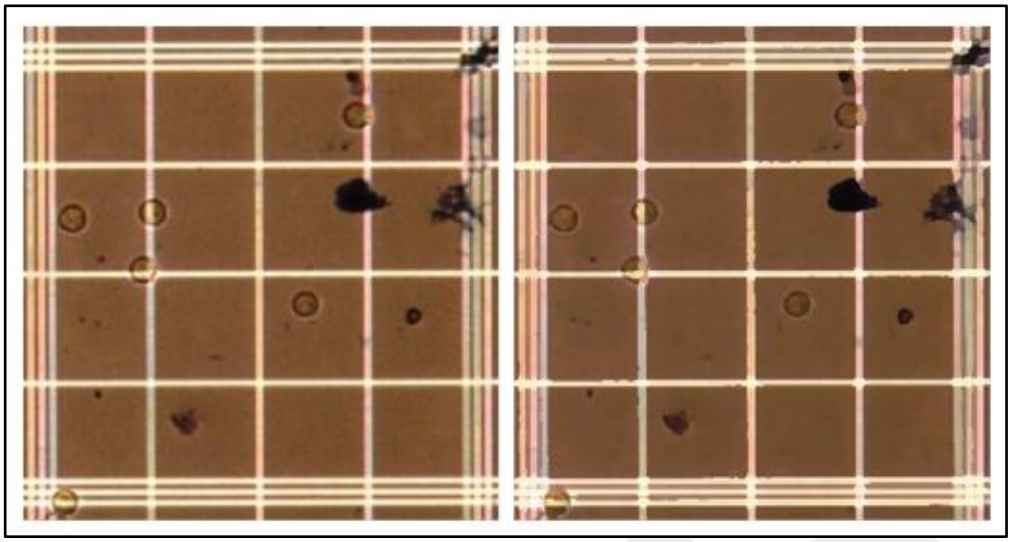

Figure 8. Sample (10x magnified objective) Image (left) and Kuwahara Filtered Image (right)

The Kuwahara kernel may be described as a square window whose size is given as:

$$J = K = 4L + 1 \tag{2}$$

L is an integer and its size previously selected by user. J is the height and K is the width of kernel which depends on L [37]. Figure 9 shows a Kuwahara kernel example and regions (sub quadrants) of kernel. Each region has the size of [(J+1)/2] x [(K+1)/2] while each black square represents a pixel.

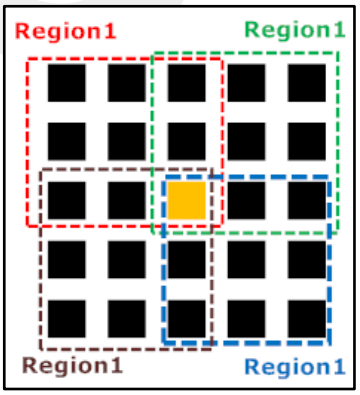

Figure 9. Kuwahara kernel for L=1 and 4 regions.

Kuwahara algorithm has the following steps;

- Select kernel size (L)
- Calculate the mean and variance for four sub quadrants
- Set the center pixel, to the mean value of the region with the smallest variance

3.2. Edge Detection

Edge may define as side that is between an object and background. Commonly used edge detection algorithms [38] are Canny, Sobel, and Laplace. Each of them has its own advantages while finding edges.

Edge detection step is very critical step, because performance of this step will affect the following steps directly. If we lose some of the edges while we finding edge, Hough transform will not work properly.

Images have some unequal lightings (lighter or darker) and also non-uniform illumination. To overcome these drawbacks and increase the accuracy of the edge detection we use the RGB's color components separately. As can be seen in Figure 10, Canny edge [39] detector is applied to each of three color components one by one and then edged images are added.

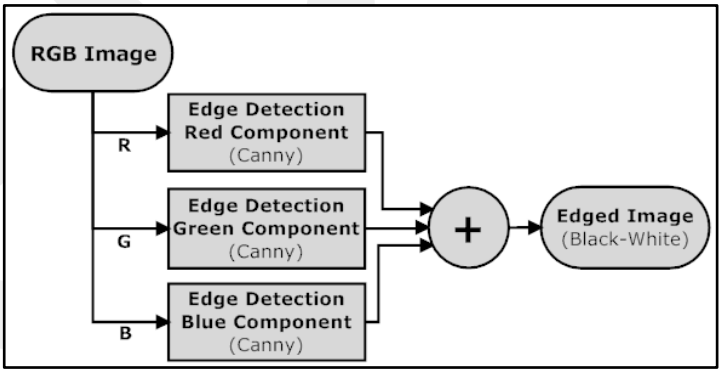

Figure 10. Edge detection algorithm which is used by the proposed method.

3.2.1. RGB Color Space and Canny Edge Detection

RGB color space can be explained based on the visible spectrum of human visual system [40]. In short, RGB color space defines color with respect to mixture of red, green, and blue color. All the used images taken from microscope with the help of the CCD camera are in RGB color space.

Canny edge detection uses the gradient magnitude to expose the potential edge pixels and reduce the effect of them through no maximal suppression and hysteresis thresholding [1]. Canny edge detection algorithm has some advantages; it has low error rate which means that it brings out the edges and does not responses to nonedges. In addition, edge points are well localized and it has only one reaction to a single edge.

3.3. Hough Transform

The Hough Transform is the segmentation method that depends on the object shape. The Hough Transform is first used to detect the straight lines [41]. Afterwards, it is extended to detection of circular shapes [42]. Although it requires a lot of memory and long computation time, it is tolerant to noise. It may work even if the pattern is corrupted or incomplete.

3.3.1. Circular Hough Transform

As we discussed before, CHT is the generalized form of HT. Since the cells have almost circler shape, we focus on CHT. As seen in Figure 11, the idea of the Hough Transform is to map each pixel from image space to a parameter space. Parameter space is also called vote space.

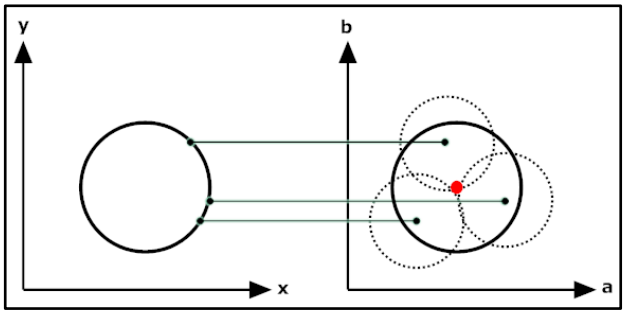

Figure 11. Image space (right) to Hough space (left) in two dimension

The total number of circles, which passes through coordinates of each edge point, is kept in an array. This array is called "accumulator array". Pick points can be detected in Hough space by using this array [43, 44]. Also the array is limited for the predefined radius sizes.

Figure 12 shows usage of accumulator array where the brighter spots are possible circle centers. First image is the original black-white input image, when we select radius size of 6 pixels we may easily see two brighter spots as pick points. Using these points and known radius size (6 pixels for little circles) locations of the two little circles are determined. Same procedure may follow for the big circle but this time radius size has to be selected as 18 pixels.

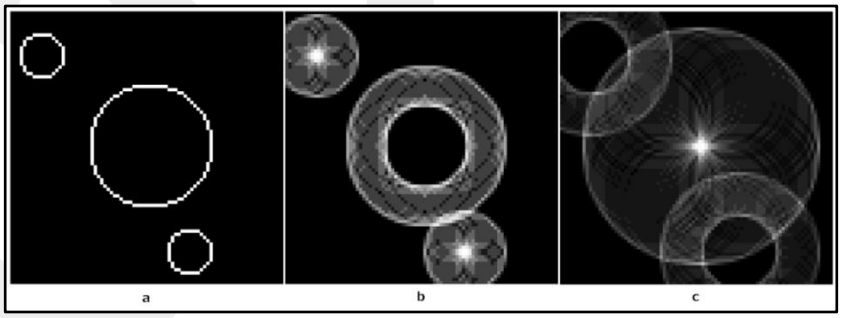

Figure 12. a) Original edged image b) Pick points at radius 6, small 2 circles detected c) Pick point at radius 18, big circle detected

From the perspective of mathematical definition of HT; implicit circle equation is defined;

$$(x-a)^2 + (y-b)^2 = r^2 \quad (3)$$

where a and b are the center coordinates of the circle and r is the radius. The parametric equation of circle is;

$$x = a + r\cos(\Theta) \quad (4)$$

$$y = b + r\sin(\Theta) \quad (5)$$

where the Θ is a parametric variable and it's the range of 0 to 2π. Parameter space for a circle will be three dimensional spaces for unknown radius (Figure 13), as a result of (4) and (5).

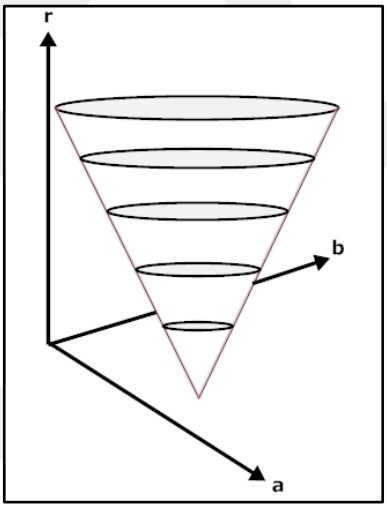

Figure 13. Circles with unknown radius, each r values have it's a and b value.

If the radius (r) is known then center of the circle is located using two dimensional mapping [45]. Also specified radius range reduces processing time and increases consistency.

3.3.2. CHT and Elimination of Overlapping Cells Areas

Hough Transform takes three parameters as a black box (Figure 14). First parameter is black-white input image that may include circular patterns. Other two parameters are minimum radius size and maximum radius size.

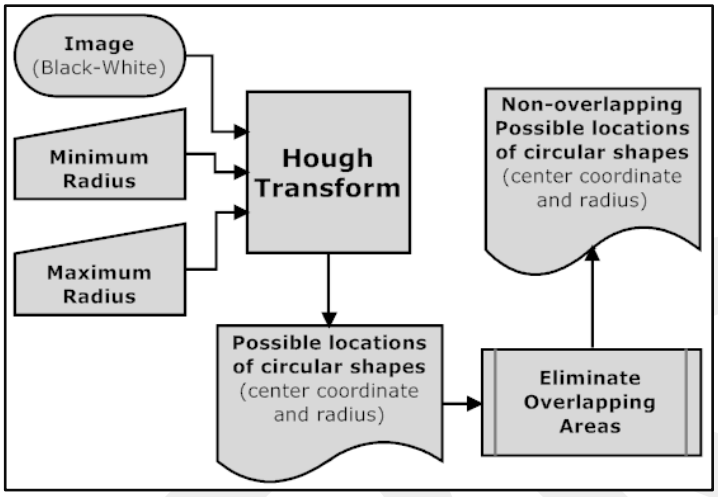

Figure 14. Hough Transform that used by the proposed method.

In this study, we obtain minimum and maximum radius empirically. 10x objective images have cells with the radius from 5 to 20 pixels. 40x objective images have cells whose radius varies from 20 to 45 pixels.

Hough Transform returns a list which contains possible circular patterns as the form of center coordinates and radius listed each row. Also there is one value added as priority calculation which indicates circularity degree relative to each other. Priority is calculated as:

$$\text{Priority value} = \text{point count} / (2 \times \pi \times \text{found radius}) \quad (6)$$

“Point count” addresses the number of circles passing through pick point while drawing circles in Hough space. Found radius is previously defined radius value. For example; Figure 12 (c), there is one pick point that corresponds to the center of the circle with radius 18 and pick count value 62. Hence priority value is 0,5482.

Each suggested cell location may be viewed as a bounding box to ease overlapping algorithm. All bounding boxes have equal dimensions with the size of corresponding circle's diameter (Figure 15).

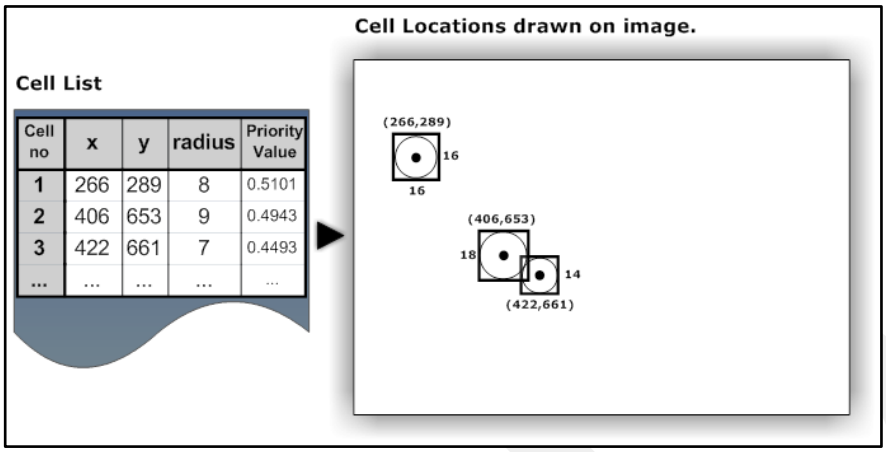

Figure 15. Cell list to cell location as bounding box

Hough transform suggests so many possible circular locations as seen in Figure 16(b). If all these possible locations are sent to ANN, overall accuracy rate is getting low. For this reason the output of Hough transform is processed for eliminating overlapping points. Figure 16 (c) shows the image with eliminated boxes.

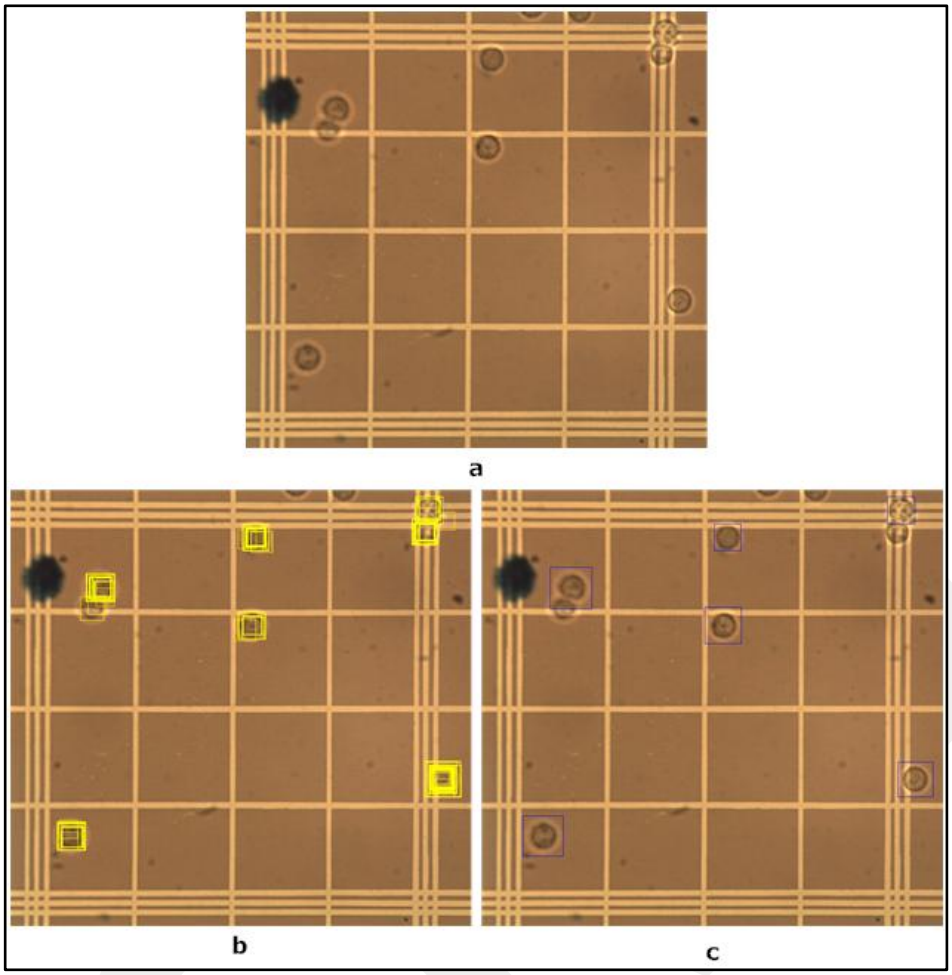

Figure 16. a) Original image b) Hough transform output without eliminate overlapping areas c) eliminate overlapping areas.

The flowchart of elimination of overlapping areas is illustrated in Figure 17. First of all, one of the elements is selected from the list and then compared with other elements one by one until the overlapping take places. When the overlapping occurs there are two possibilities left; one bounding box may cover another or two bounding boxes intersect one another. If the one covers another, the inner one is removed from the list. If the two of them meet, one with less priority value is removed from the list which has less priority value. This process repeats until the all collusions end.

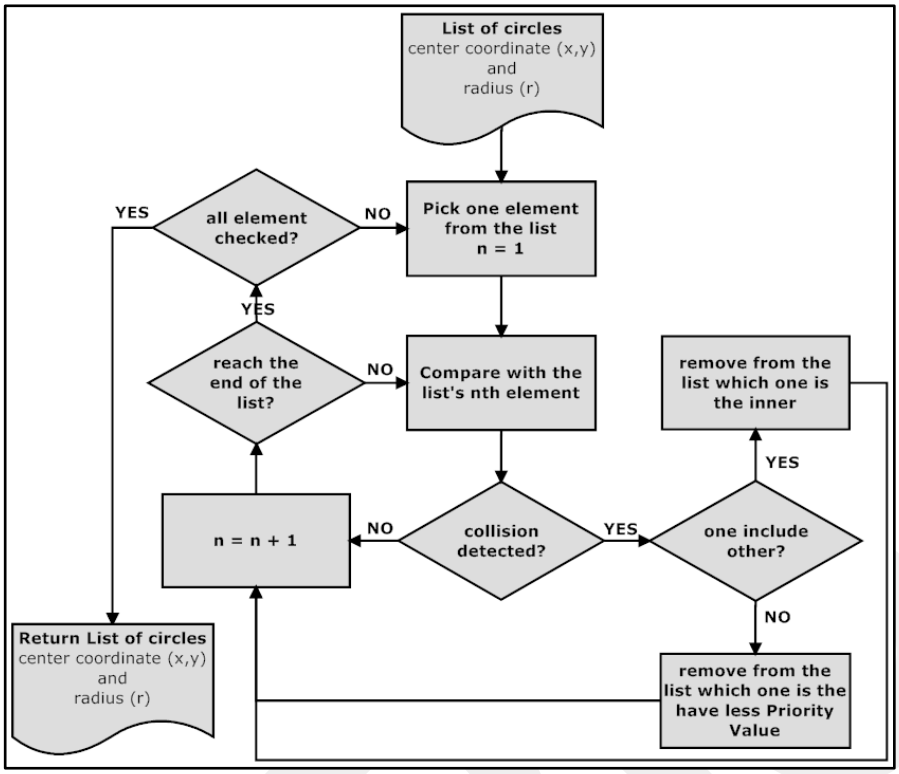

Figure 17. Elimination of overlapping areas

CHAPTER 4

CLASSIFICATION OF CELL IMAGES

In pattern recognition, classification is referred to as a decision making process that appoint a given input data into one of the given categories. First thing for the classification of given data is learning process. When the learning process ends, classification may be achieved.

Learning method types are divided into supervised, unsupervised, reinforcement, and evolutionary learning. Supervised learning is widely used in pattern recognition [46]. In the supervised learning a set of training examples (training data) and corresponding correct responses (target data) are provided and then supervised learning algorithm produced inferred function.

Artificial Neural Network is used as a classifier for two reasons; first reason is distinguish cell images from non-cell images to define cell count. Second, it is used to make decision alive and dead cell images. Figure 18 summarizes the entire classification procedure.

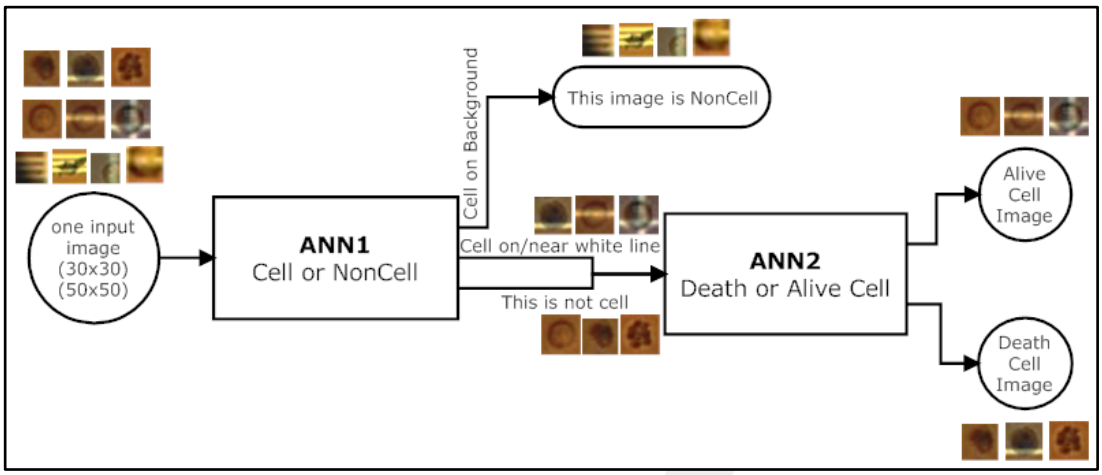

Figure 18. Generally Classification Step

4.1. Artificial Neural Network

Artificial neural networks (ANN) are the computational simulation form of the microstructures of a biological nervous system. In another words, imitate nerve cells with the mathematical representation. In 1940s, McCulloch and Pitts [47] found first mathematical neuron model for performing logic functions. Early 1960s, Rosenblatt [48] came with the perceptron idea which is consisting of more than one neuron. Today, ANN is used widely for optimization problems, control problems, industrial applications and classification issues.

ANN has two abilities which are consistent with our classification needs.

- Generalization; the ability of producing suitable outputs for inputs which are not encountered during training (learning)
- Nonlinear nature; convenient even for nonlinear problems

4.1.1. Neuron Model

A neuron is a main building block of ANN. Figure 19 shows the block diagram of the neuron. A neuron has three main parts: synapses, connected the input signal (X_n) to the neuron by a set of weights (W_k); Adder, sums up input signals which is weighted by the respective synapses of neuron; and an activation function $\phi(v_k)$ for limit the amplitude of neuron output. Also, bias (b_k) is sometimes applied to increase or decrease the output of the neuron [49].

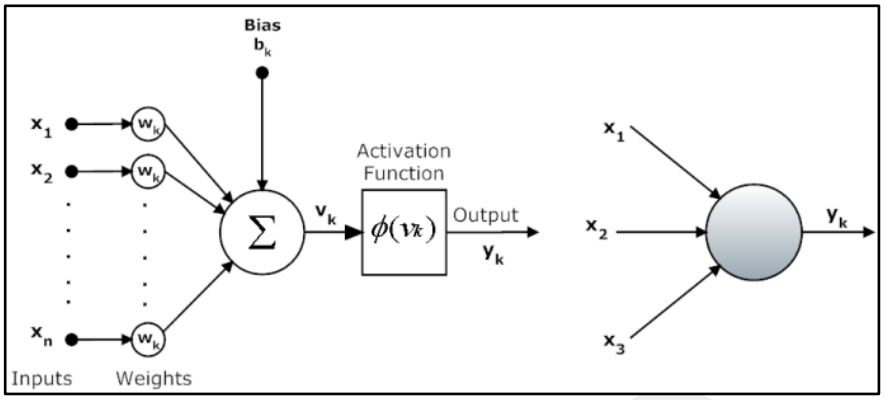

Figure 19. Model of a neuron and Symbol of a neuron

Mathematical representation of neuron is:

$$v_k = \sum_{j=1}^{n} w_{kj} \, . \, x_j \tag{7}$$

$$y_k = \phi(v_k + b_k) \tag{8}$$

where:
$x_1, x_2, x_3, \ldots, x_n$ are the input signals,
$w_{k1}, w_{k2}, \ldots, w_{kn}$ are the weights for neuron k,
b_k is the bias,
v_k is the adder or the linear combination of input signal,
ϕ (v_k) is the activation function,
y_k is the output signal of the neuron.

The output range depends on activation function. Figure 20 presents some activation functions.

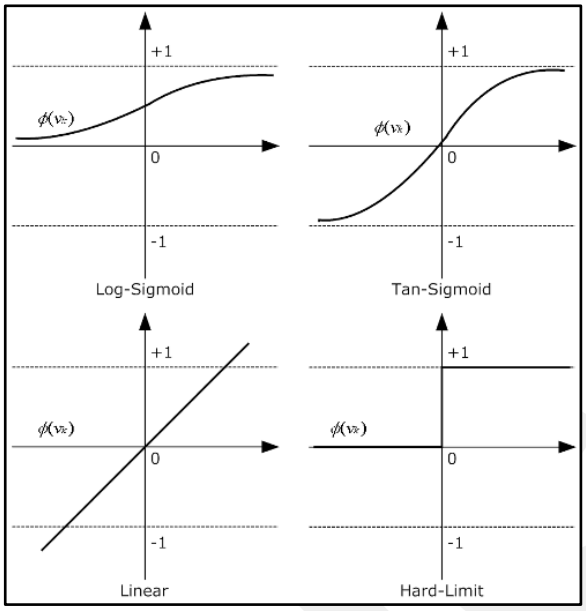

Figure 20. Activation Functions

Hard-Limit activation function is (9);

$$y_k = \begin{cases} 1, & if\ vk \geq 0 \\ 0, & if\ vk < 0 \end{cases} \tag{9}$$

Log-sigmoid activation function is (10);

$$y_k = \frac{1}{(1+e^{-vk})} \tag{10}$$

Tan-Sigmoid activation function is (11);

$$y_k = \tanh(vk) \tag{11}$$

Linear activation functions; reproduce response for the input as the output itself.

4.1.2. Perceptron

The perceptron is the plain form of a Neural Network. As seen in Figure 21, it consists of only output layer that is directly connected to the input layer.

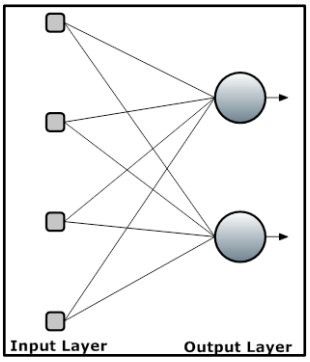

Figure 21. Perceptron

Perceptron may classify only linearly separable classes. Linearly separable means that the input data or the given data can be distinguished correctly with a linear decision boundary [50]. Since the black and white circles are two different groups of data on Figure 22, first group of data in (a) can be separated by a strict line (dashed) but second group of data in(b) cannot be separated by a line.

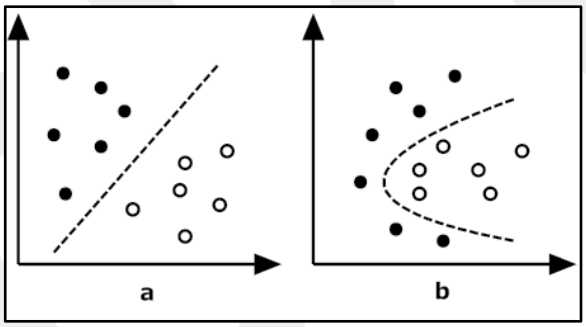

Figure 22. Linearly (a) and Non-Linearly (b) Separable data in 2d

4.1.3. Multilayer ANN

Linear separable issue limits the perceptron. To extend capability of perceptron, basic idea is layered version of it. Multilayer neural network has one output layer and one or more hidden layer (Figure 23). Increasing the hidden layer gives the ability of non-linear classes' separation.

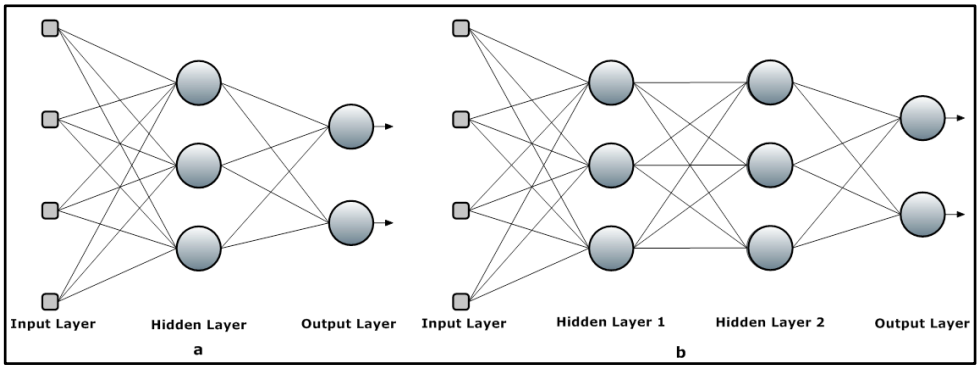

Figure 23. Multilayer ANN with 1hidden layer (a) Multilayer ANN with 2 hidden layers

4.1.4. Feed-Forward, Back-Propagation and Training (Learning) ANN

ANN learns by example, accordingly, what is needed is a set of examples that are representative of all possible variations of the cells. This example set, also called training set which consists of sample inputs (input data) and corresponding outputs (target data) for all these inputs.

Training of ANN expresses calculation of optimum weights (W_k) for all neuron connections with respect to training data. Figure 24 shows the process of learning that has two phases; forward-pass (feed-forward) and backward-pass (back-propagation).

In the forward pass, one example (one element of training set) is presented to the ANN and its effect propagates through the network neuron by neuron until the output is produced. During the forward pass weights are fixed.

On the phase of backward pass, all weights are updated in according to error-correction. Error is the difference of the actual output and desired (targeted) output. This error signal propagated backward through the network, all weights are updated to get close the target value. This oscillation repeats until optimum weights are obtained [51].

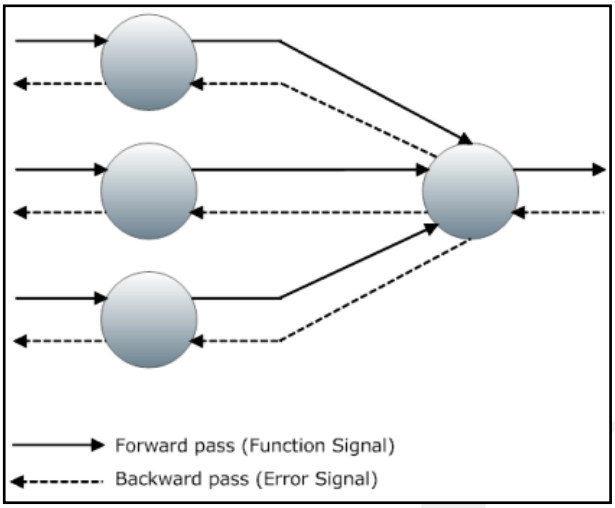

Figure 24. Feed-forward (straight lines) and Backpropagation (dashed lines)

Also there is a test data set to measure how effectively the ANN trained. ANN training success is measured by its generalization ability. To improve this capability sometimes amount of hidden layer or neuron number of hidden layer may be changed. There is no rule to define appropriate numbers for all these cases. Optimum numbers vary problem to problem.

4.2. Usage of ANN

Proposed method uses 3 layered (1hidden and 1output) feed-forward back propagation ANN. The number of neuron in hidden layer is set to 100 empirically. At the beginning of the classification, test and training data sets are created using completely different cell images. Images are resized with 50x50 pixels for 40x objective images and 30x30 to 10x objective images. After the dimensions of all images are equalized, histogram equalization is applied to each image for reduce the effect of light difference. There is no feature extraction step for data sets. Instead, the pixel values are used as features.

Assessment of cell images is a first step of cell viability classification. ANN1 has been trained for three responses with respect to input image: cell on background, cell on/near white line, and non cell. Figure 26 (a) shows the example of training data.

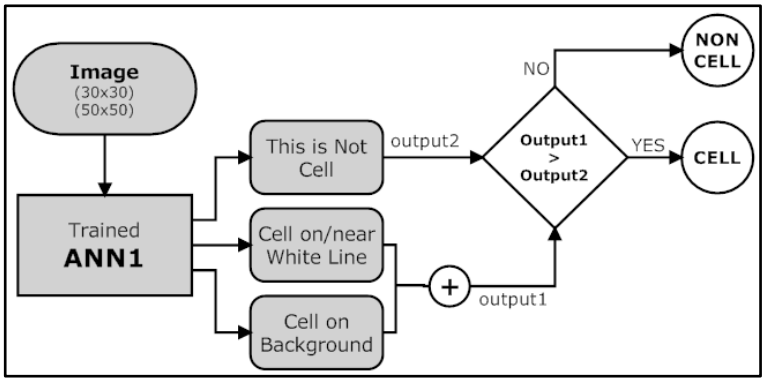

Figure 25. ANN1- Distinguish cell from non-cell images.

Figure 25 outlines the cell – non-cell decision making process. Crucial part is to divide the cells into two classes. If the first output of ANN1 (This is not cell) is less than the sum of the other two outputs, the input image is assumed to be cell. Otherwise, given image is not a cell.

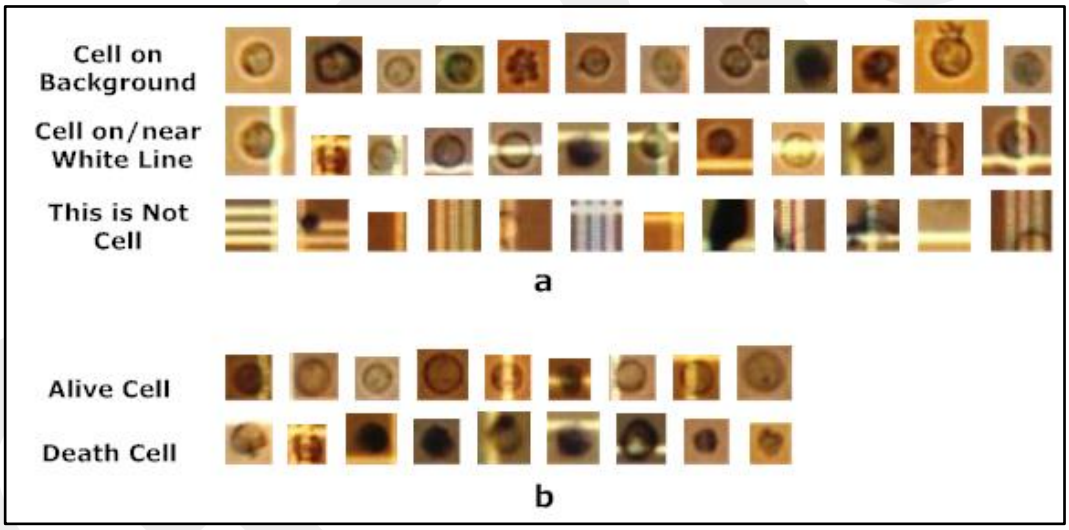

Figure 26. Examples of Training Data for ANN1(a) and for ANN2(b)

After distinction phase of cells from non-cells, all cell images are inputted to the second decision making process which decides whether the cell is alive or dead (Figure 27).

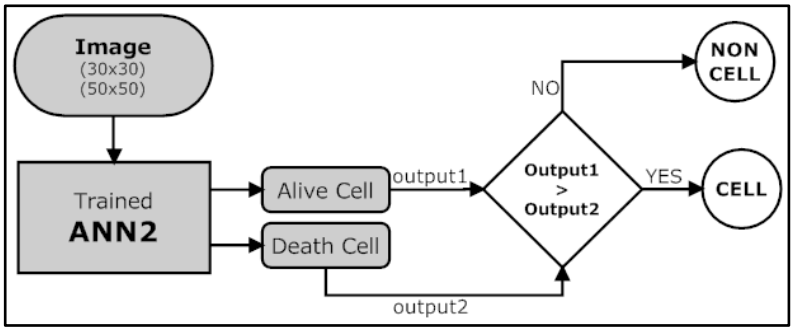

Figure 27. ANN2 – Distinguish alive cells from death cells.

CHAPTER 5

EXPERIMENTAL RESULTS AND DISCUSSIONS

In this study, experimental results are introduced via two measures: success rate of sensitivity of finding the cell location and success of total cell count performance on the basis of alive and dead cells count [52].

Manual cell counting results may show major changes of cell count by examiner to examiner. Therefore, manual counting test group is divided into two, according to their experience level as experts and non-experts. Expert group has 2 participants with highly experienced. Non-expert group consists of 3 examiners with moderate level practiced.

Table 1 shows all results as a tabular form. Manual counting of expert and non-expert have over 10% standard deviation themselves but when all these two group results combined, this time overall standard deviation increases over 20%. This variation between manual counting results is the proof of manual counting differentiation of examiner to examiner which is mentioned before. Although manual counting results are not strictly consistent, proposed system is produced outputs close to all manual counting results as much as possible.

Table 1. Statistical results of alive and dead cell by comparing the count results of experts and non-experts.

	Total Manuel Count Nonexpert (n=3)		**Total Manuel Count Expert (n=2)**		**Total Manuel Count Expert+Nonexpert (n=5)**		**Autometed count under 40x**		**Autometed count under 10x**	
	Alive	***Death***	***Alive***	***Death***	***Alive***	***Death***	***Alive***	***Death***	***Alive***	***Death***
Test Image 1	32,33 ±2,05	6,67±4,64	27,5±3,50	14,5±2,50	30,4 ± 3,61	9,8±5,492	31	7	21	6
Test Image 2	58±7,26	7±1,63	45,5±12,50	27±15,00	53 ± 11,47	15±13,70	61	19	23	15
Test Image 3	68,67±2,87	13,67±3,77	61±1,00	27±2,00	65,6±4,41	19±7,27	76	40	30	24
Test Image 4	29±0,82	4,33±0,94	27,5±2,50	9,5±2,50	28,4±1,85	6,4±3,07	36	8	8	11
Test Image 5	51±7,79	15,67±2,62	46,00± 1	25±3	49,00±6,54	19,4±5,35	42	9	25	36

Figure 28 and Figure 29 show alive and dead cell counting results for 5 different test images, respectively. Each of the test images taken from CCD camera consists of all possible adverse conditions such as different light condition and different cell suspension dilation. Also these test images include dead and alive cells.

Each bar indicates number of cell count for one test image. While M1, M2, and M3 are the non-experts and M4 and M5 are the experts. A40 and A10 point out automatic cell count results with respect to 40x magnified objective and 10x magnified objective.

Figure 28 and Figure 29 indicates only the number of manual counting without standard deviation. As seen those tables, each manual counting results are varies examiner to examiner. Success rate of proposed algorithm is changes with the depends on examiner.

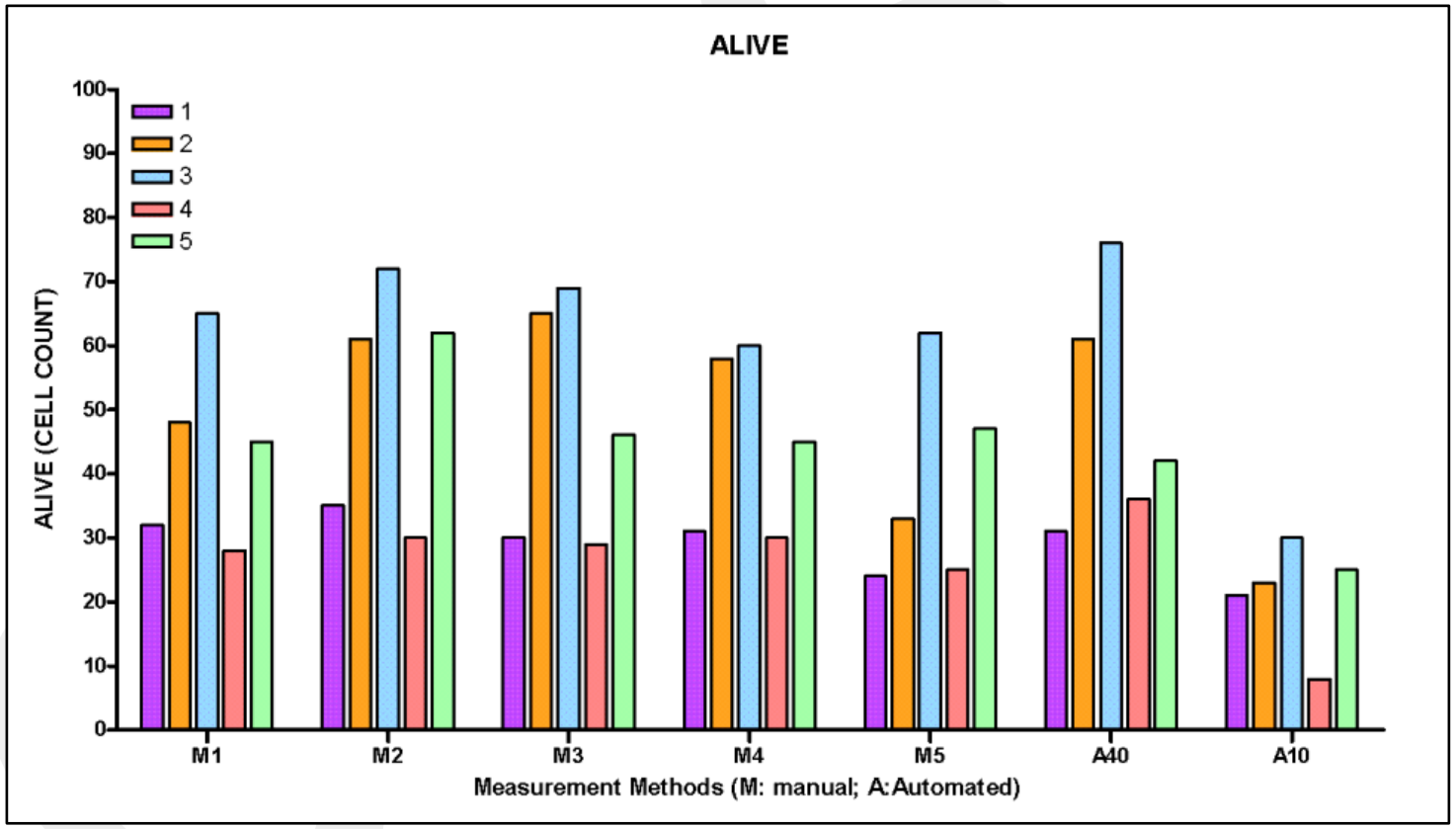

Figure 28. Comparison of manual and automated alive cells count. M1 through M5 are the result of manual counts, A40 and A10 are the results of automated counts with 40x and 10x magnified images respectively.

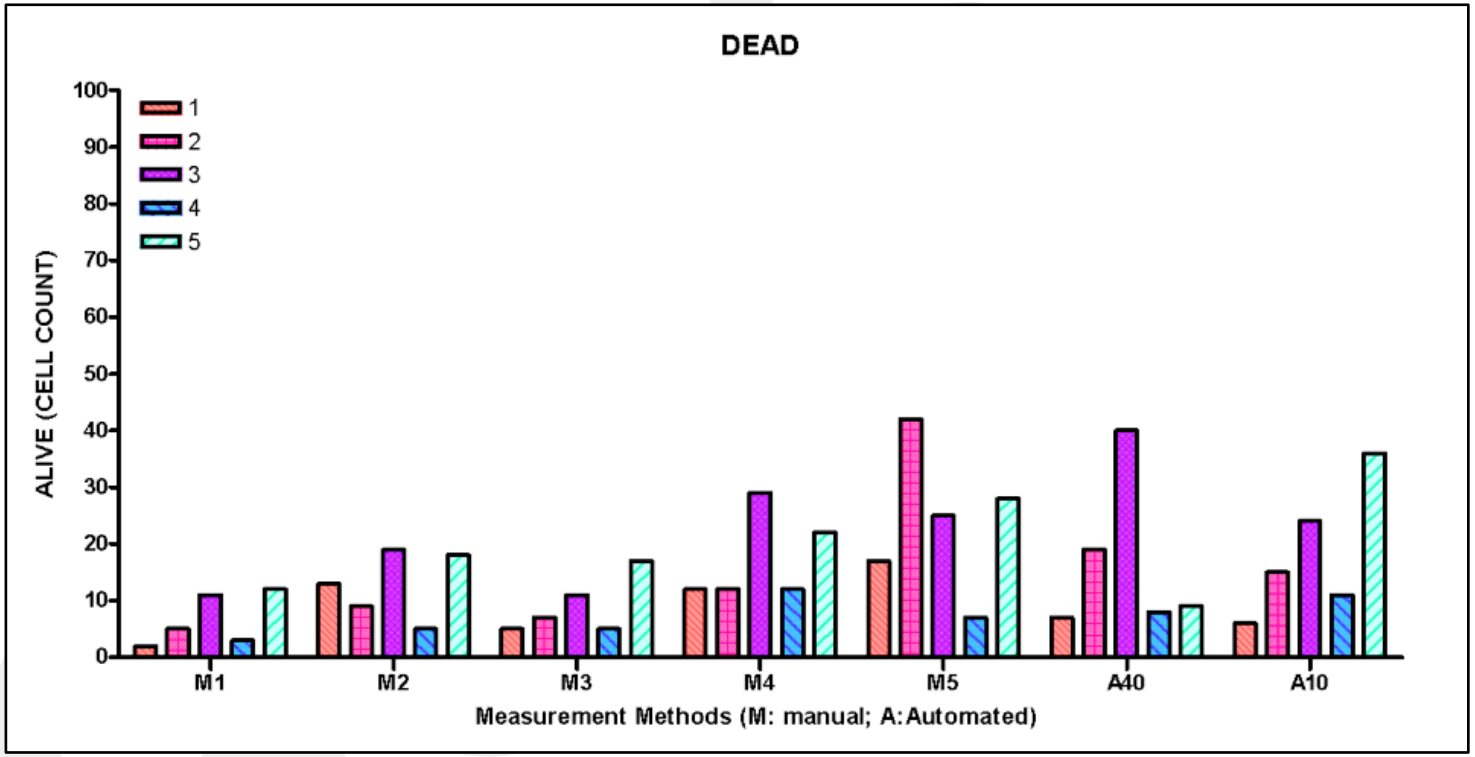

Figure 29. Comparison of manual and automated dead cells count. M1 through M5 manual counts, A40 and A10 automated counts with 40x and 10x magnified images, respectively.

In order to measure the performance of neural networks, confusion matrices are formed. A Confusion matrix is the way of representing consistency of produced output results. The form of such a matrix is given in Table 2. True positives (TP), true negatives (TN), false positives (FP), and false negatives (FN), are the four different possible outcomes of a single prediction for a two-class case. A false positive is when the computed value is incorrectly classified as negative, when it is in fact positive. A false negative is when the computed value is incorrectly classified as positive when it is in fact negative. True positives and true negatives are obviously correct classifications. In addition, "*Specificity*" measures the proportion of negatives which are correctly identified and "*Accuracy*" can be seen as the degree of closeness of measurements. "*Positive predictive value*" measures the probability that a positive result is truly positive and "*Negative predictive value*" evaluates the probability that a negative result is truly negative.

Table 2. Form of confusion matrix.

		Computed		
		Positive	**Negative**	
Desired	**Positive**	True Positive (TP)	False Positive (FP)	*Positive predictive value* = TP/(TP+FP)
	Negative	False Negative (FN)	True Negative (TN)	*Negative predictive value* = TN/(FN+TN)
		Sensitivity =TP/(TP+FN)	*Specificity* =TN/(FP+TN)	

Success rates of training set are given in Table 3. This table indicates how well the ANN1 and ANN2 learn. ANN1 is trained using 1774 10x cell / 1522 10x non-cell images and 420 40x cell/395 40x non-cell images. ANN2 is trained using 302 10x alive/86 10x death cell images and 324 40x cell / 149 40x non-cell images.

Table 3. Training set confusion matrices for 10x and 40x magnified images

10x Cell/Non-Cell Traning				
		Computed		
		Cell	**Non-cell**	
Desired	**Cell**	1757	17	*99%*
	Non-cell	49	1473	*97%*
		97%	*99%*	

10x Alive/Death Traning				
		Computed		
		Alive	**Death**	
Desired	**Alive**	289	13	*96%*
	Death	3	83	*97%*
		99%	*86%*	

40x Cel/Non-Cell Traning				
		Computed		
		Cell	**Non-Cell**	
Desired	**Cell**	414	6	*99%*
	Non-cell	3	392	*99%*
		99%	*98%*	

40x Alive/Death Traning				
		Computed		
		Alive	**Death**	
Desired	**Alive**	304	20	*94%*
	Death	11	138	*93%*
		97%	*87%*	

The proposed study has two parts and the first part is finding location of cells using input image. Table 3 and Table 4 illustrate the performance cell/non-cell classifier by forming confusion matrix. As can be seen from tables, the entry of non-cell/non-cell is left empty on purpose because each of the underlying images consists of many possible candidates for non-cells. If those candidates are taking into consideration, they degrade the statistical results of specificity and negative predictive value and therefore make them meaningless. Secondly, Table 5 and Table 6 show the success rate of alive and death cell separation from found cell locations.

Table 4. Cell and Non-cell confusion matrices of test set for 10x magnified objective images.

Test Image 1 - 10x				
		Computed		
		Cell	**Non-cell**	
Desired	**Cell**	23	20	*53%*
	Non-cell	4	-	
		85%		

Test Image 4 - 10x				
		Computed		
		Cell	**Non-cell**	
Desired	**Cell**	19	19	*50%*
	Non-cell	0	-	
		100%		

Test Image 2 - 10x				
		Computed		
		Cell	**Non-cell**	
Desired	**Cell**	37	38	*49%*
	Non-cell	1	-	
		97%		

Test Image 5 - 10x				
		Computed		
		Cell	**Non-cell**	
Desired	**Cell**	41	25	*62%*
	Non-cell	20	-	
		67%		

Test Image 3 - 10x				
		Computed		
		Cell	**Non-cell**	
Desired	**Cell**	49	35	*58%*
	Non-cell	13	-	
		79%		

Total of 5 Test Images - 10x				
		Computed		
		Cell	**Non-cell**	
Desired	**Cell**	169	137	*55%*
	Non-cell	38	-	
		82%		

Table 5. Cell and Non-cell confusion matrices of test set for 40x magnified objective images.

Test Image 1 - 40x				
		Computed		
		Cell	**Non-cell**	
Desired	**Cell**	35	6	*85%*
	Non-cell	5	-	
		88%		

Test Image 4 - 40x				
		Computed		
		Cell	**Non-cell**	
Desired	**Cell**	34	2	*94%*
	Non-cell	8	-	
		81%		

Test Image 2 - 40x				
		Computed		
		Cell	**Non-cell**	
Desired	**Cell**	63	9	*88%*
	Non-cell	17	-	
		79%		

Test Image 5 - 40x				
		Computed		
		Cell	**Non-cell**	
Desired	**Cell**	39	22	*64%*
	Non-cell	14	-	
		74%		

Test Image 3 - 40x				
		Computed		
		Cell	**Non-cell**	
Desired	**Cell**	75	5	*94%*
	Non-cell	33	-	
		69%		

Total of 5 Test Images - 40x				
		Computed		
		Cell	**Non-cell**	
Desired	**Cell**	246	44	*85%*
	Non-cell	77	-	
		76%		

Table 6. Alive and Death cell confusion matrices of test set for 10x magnified objective images.

Test Image 1 - 10x				
		Computed		
		Alive	**Death**	
Desired	**Alive**	17	3	*85%*
	Death	1	2	*67%*
		94%	*40%*	

Test Image 4 - 10x				
		Computed		
		Alive	**Death**	
Desired	**Alive**	5	10	*33%*
	Death	3	1	*25%*
		63%	*9%*	

Test Image 2 - 10x				
		Computed		
		Alive	**Death**	
Desired	**Alive**	17	13	*57%*
	Death	4	3	*43%*
		81%	*19%*	

Test Image 5 - 10x				
		Computed		
		Alive	**Death**	
Desired	**Alive**	8	19	*30%*
	Death	7	7	*50%*
		53%	*27%*	

Test Image 3 - 10x				
		Computed		
		Alive	**Death**	
Desired	**Alive**	19	14	*58%*
	Death	4	12	*75%*
		83%	*46%*	

Total of 5 Test Images - 10x				
		Computed		
		Alive	**Death**	
Desired	**Alive**	66	59	*53%*
	Death	19	25	*57%*
		78%	*30%*	

Table 7. Alive and Death cell confusion matrices of test set for 40x magnified objective images.

Test Image 1 - 40x				
		Computed		
		Alive	Death	
Desired	Alive	29	1	*97%*
	Death	3	2	*40%*
		91%	*67%*	

Test Image 4 - 40x				
		Computed		
		Alive	Death	
Desired	Alive	22	3	*88%*
	Death	6	3	*33%*
		79%	*50%*	

Test Image 2 - 40x				
		Computed		
		Alive	Death	
Desired	Alive	49	2	*96%*
	Death	3	9	*75%*
		94%	*82%*	

Test Image 5 - 40x				
		Computed		
		Alive	Death	
Desired	Alive	25	3	*89%*
	Death	7	4	*36%*
		78%	*57%*	

Test Image 3 - 40x				
		Computed		
		Alive	Death	
Desired	Alive	50	7	*88%*
	Death	3	15	*83%*
		94%	*68%*	

Total of 5 Test Images - 40x				
		Computed		
		Alive	Death	
Desired	Alive	175	16	*92%*
	Death	22	33	*60%*
		89%	*67%*	

Throughout this study our work is started with the investigation of the images under 40x magnified objective first and then it is extended to 10x. The proposed method is tested on different images obtained from the same cell line HL-60 in different dates with different dilutions.

Including with the perfectly visualized images test set of images also have all the possible variety of adverse conditions such as; deformed cell shape, images with different brightness, single cell image with unequal brightness, the images not focused well, images having clumped cells and impurities in cell suspension. Figure 30 shows some of the cell images. Any image under investigation having any of these unwanted situations makes the automated cell counting process harder and unreliable.

HL-60 cells usually have circular shape, but their shapes may change depending on the conditions of the cell culture. Generally, death cells have much more shape deformation than alive cells. In addition, cells may be located over the white lines which are found default on a Hemocytometer. Shape deformation influences the proposed cell counting method directly and this is the most crucial step for the success of Hough transform.

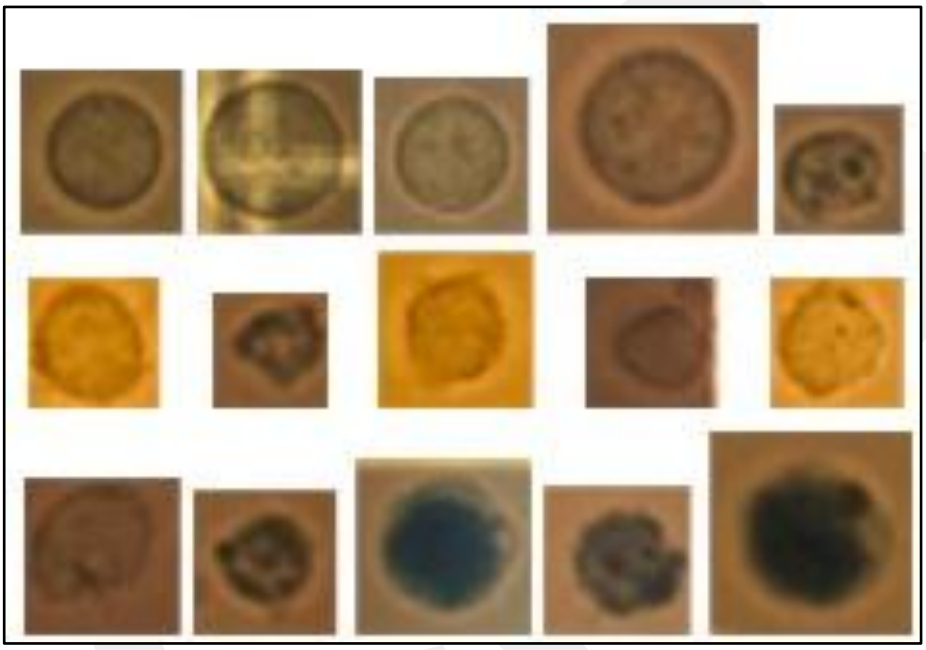

Figure 30. Images of HL-60 cell used in the study with different possible variables

There may be two possible reasons for the brightness differences; first, the variation in the adjustment of the light source of the microscope. The light intensity is adjusted by the user manually by means of the slider controller part of the microscope. Figure 31 is shows slider control unit. Since the brightness is controlled manually, the intensity of the light passing through the image may not be stable so that the variable brightness is resulted from image to image. Second reason is because of the hemocytometer itself. Hemocytometer is a glass based commercially produce microscope slides and produced by different companies. Each hemocytometer from different companies refracts light differently. Finally due to these two possible reasons brightness of the images varies which then affects the success of the edge detection and training of ANN.

Figure 31. Slider control unit for the light power of microscope.

The unequally shining of images under microscopy is the main problem especially working with 10x magnified images. Because of the poorness of slider control unit light do not illuminate the whole slide which in turn makes some parts of images brighter and some parts darker. Due to this problem edge detection step is negatively affected during processing the input images. Figure 32 illustrates brightness difference in the counting area, presence of clumped cells, and existence of impurities.

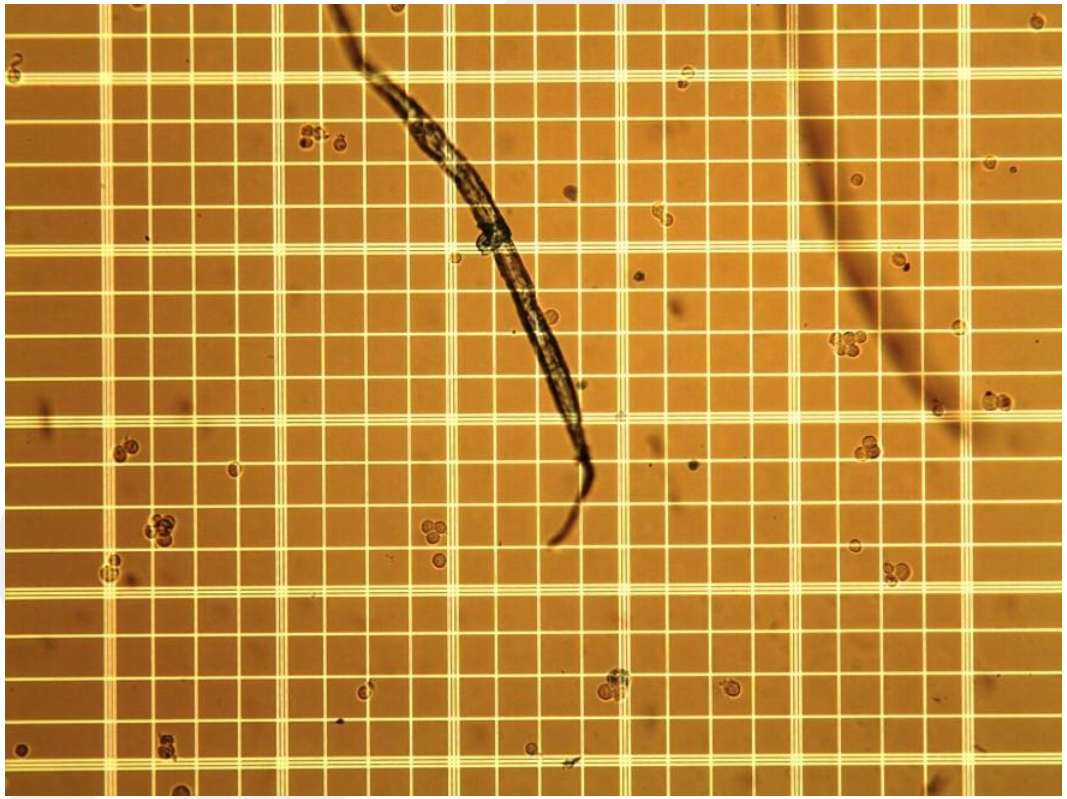

Figure 32. The image containing the examples of brightness difference in the counting area, presence of clumped cells, existence of impurities; unwanted cell or dye residuals and view of the white lines on the hemocytometer.

In order to get the best visual condition while working with microscope the researcher has to be tuned the microscope by setting the course and fine adjustment wheels. If the microscope is not adjusted well the image is blurred. The blurred image changes the researchers' perception on the basis of the appearance of cells so the success rate of ANN decreases. Figure 33 shows the images captured from microscope that is not adjusted well.

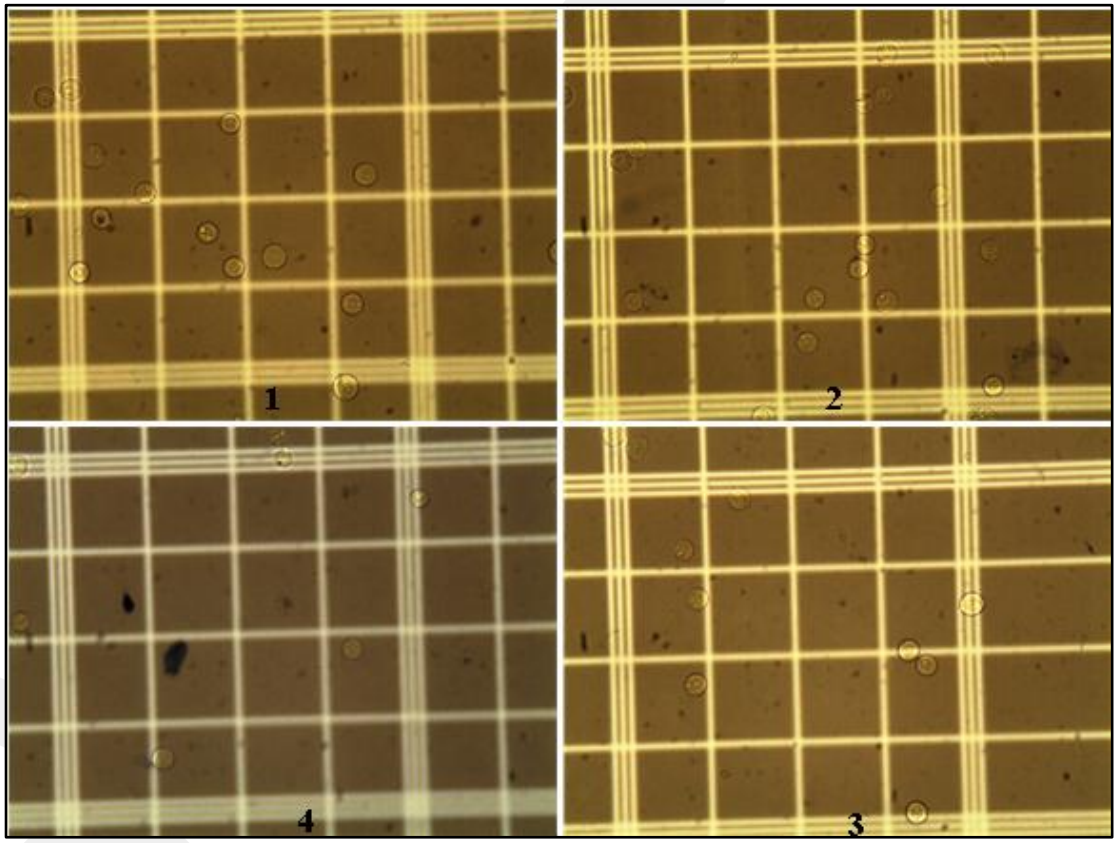

Figure 33. The images containing the examples of pictures in which the microscope is not adjusted well and resulted in the blurred object at a various ranges from 1 to 4.

Cells are adherent while they are dividing and they are assumed as an individual big, elliptical cell. In addition, death cell precipitate in some images, cell suspension contains different partials like; trypan blue stain residuals due to insufficient clean on the Hemocytometer surface. Due to these two parameters the performance of ANN and Hough transform decreases.

Experimental results are given in two titles: first, success rate of cell location finding in terms of sensitivity and second, general performance evolution of proposed method for cell viability.

CHAPTER 6

CONCLUSIONS AND FUTURE WORK

In this study, until the step in which the cells are counted digitally we chose, tried and decided to use or not use several methods. The image processing step is started with 40x magnified images of HL-60 cells first and the study is extended to the 10x magnified images.

At the first trial, since the white lines on the hemocytometer made the digital count difficult we decided to erase these lines from the input images by synchronizing the value of background color with the white lines. At the end, the white lines are eliminated but the cells on these lines either.

To determine the location of the cells on the input image with the histogram thresholding, the morphological operators like dilation, erosion and opening are used. In this trial due to brightness and hue difference of cells, the efforts finding the location of cells failed. The images chosen to determine threshold which is necessary for determination of histogram thresholding showed differences in refracting the light so that the optimum value was not determined to be applied to all input images.

For segmentation of images Watershed algorithm is also used. Since the cells are closely located to the white lines of hemocytometer this attempt is failed either. Thereupon region growing algorithm was used, but again it is failed due to the close location of cell and white lines.

HL-60 cells have spherical shapes so that Hough transform, which is the algorithm, used to determine spherical shapes was tried. Since Hough transform can identify pattern using black-white images, almost all fundamental edge detection algorithms such as Sobel, Prewitt, and Canny were tried together with Hough transform one by one. At the end of all these trials, the combination of canny algorithm and Hough transform is found to be successful.

Since 10x and 40x magnified objects have different light intensity; the brightness normalization is tried by using histogram stretching, but it was unsuccessful again. To get rid of the difference in light intensity of the images different color spaces were used such as HSV, YUV but it was unsuccessful either.

Brightness differences on the images especially for 10x magnified ones, the obtained RGB input images are divided into to the components; red, green, blue. The canny edge detection is applied to each component and by this way the negative effect of light intensity difference on edge detection is decreased.

In order to differentiate cells from non-cells and deaths from alive cells, the neural network was used. In the cell/non-cell differentiation part, the neural network with 2-output representing cell and non-cell classes was used initially. Owing to poor performance of the system, the initial network was replaced with the one with 3-output representing non-cell, cells on or near to the white lines, and cells away from white lines. This resulted in raising the success rate of classification. Also all basic ANN topologies such as single layer and double layer were tested. In addition, all these topologies were tested with different numbers of hidden neurons to determine optimum number of hidden layer neurons.

For a better performance of overall system, input images were filtered more than once by different filters with different kernel sizes.

At the end of this study, after comparing the results of manual and automated counts including with their statistical analysis it is concluded that the proposed method for cell viability determination is more accurate in 40x than 10x magnified images.

One possible future work may be extending the types of counted cells. This thesis is used a circular shape HL-60 cells. There are various kinds of cells which are having different shape features such as, elliptical. Another future work may be trying same algorithm with better quality microscope which is used with higher-resolution CCD camera. Additionally, owned 40x and 10x magnified image database may serve public use with adding alive and death cell marking from experts. Also proposed method might test using much more images to generalize variety of statistical tools.

When 100% success rate achieved for 40x magnified images, external automatic robot arm can be designed and worked together with the proposed system. Robot arm can be connected to the microscope's stage control. System can take all 25 images automatically and process all these images for getting cell count results.

Yet another major remaining work is to review additional machine learning algorithms for increasing classifier successes such as; support vector machine (SVM) , learning vector quantization (LVQ) and radial basis function (RBF). Outcomes of these reviews might be used for developing a decision support system for viability of cells by light microscopy to help pathologies.

REFERENCES

[1] Gonzalez, R. C., Woods, R. E., "Digital Image Processing ", 2nd. Ed., 2002.

[2] Viola P., Jones M. J., "Robust Real-Time Face Detection", International Journal of Computer Vision 57(2), pp.137–154, 2004.

[3] Kwaśnicka H., Wawrzyniak B., " License plate localization and recognition in camera pictures", AI-METH 2002 – Artificial Intelligence Methods, 2002.

[4] Ionela, N.A., Monica, B., "Satellite Image Improvement using Phase Information and Wavelet Transform", Communications (COMM), 2010 8th International Conference, pp. 137-140, 2010.

[5] G. Papari, N. Petkov and P. Campisi, "Artistic edge and corner enhancing smoothing", IEEE Trans. on Image Processing, 16 (10), 2007, 2449-2662.

[6] Rajwinder Kaur, Monika Verma, Kalpna, Harish Kundra, "Classification of various edge detectors", Department of Computer Science, RIEIT, Railmajra.

[7] Mark A. Haidekker, "Advanced Biomedical Image Analysis ", John Wiley & Sons Inc., 2011.

[8] Edited by J. M. Davis, "Basic Cell Culture (Practical Approach) ", Oxford University Press, 2nd Edition, 2002.

[9] URL: http://en.wikipedia.org/wiki/Optical_microscope. Site last visited in July 2011.

[10] Tanz, W.S., Tsongalis, G.J., Lamber, W.C., "Further studies on selection for viable cells in Culture using cell sorter technology", Engineering in Medicine and Biology Society. Proceedings of the Annual International Conference of the IEEE, pp. 303-304, 1988.

[11] Mary C. Phelan, "Current Protocols in Cytometry", A.3B.1-A.3B.10, John Wiley & Sons, Inc., 1997.

[12] Wang YY., Lin CC., Sun YN., "Registration-Based Segmentation of Nerve Cells in Microscopy Images", 31st Annual International Conference of the IEEE EMBS., pp.6726-6729, 2009.

[13] Sinha, N., Ramakrishnan, A.G., "Automation of Differential Blood count", T ENCON Conference on Convergent Technologies for Asia-Pacific Region, pp.547-551, 15-17 Oct. 2003.

[14] Li-hui Zou, Jie Chen, Juan Zhang,Narciso Garcia, "Malaria cell counting Diagnosis within Large Field of View", DICTA '10 Proceedings of the 2010 International Conference on Digital Image Computing: Techniques and Applications, pp. 172-177, USA, 2010.

[15] Tobias Bergen, Dirk Steckhan, Thomas Wittenberg and Thorsten Zerfab, "Segmentation of Leukocytes and Erythrocytes in Blood smear images", 30th Annual international IEEE EMBS Conference, Vancouver, Canada, August 20-24, 2008.

[16] B. Liu, C. Yin, Z. Liu, Z. Zhang, J. Gao, M. Zhu, J. Gu, and K. Xu, "Microscopic image analysis and recognition on pathological cells", Electrical and Computer Engineering, Canadian Conference, pp. 1022-1025, 2007.

[17] Mohapatra, S., Patra, D., Satpathi, S., "Image Analysis of Blood Microscopic Images for Acute Leukemia Detection", Industrial Electronics, Control & Robotics (IECR), pp. 215 – 219, 27-29 Dec. 2010.

[18] Refai H., Li L., Teague T. K., and Naukam R., "Automatic Count of hepatocytes in microscopic images", Proc. Int'l Conf. on Image Processing, pp. 1101-1104, Sept 2003.

[19] Anoraganingrum D., "Cell Segmentation with median Filter and Mathematical Morphology Operation", Image Analysis and Processing, pp. 1043-1046, 1999.

[20] Xiao-qin Zhang, Kuo Yang, Bao-qing Hao, "Cell-Edge Detection Method Based on Canny Algoritm and Mathematical Morphology", Image and Signal Processing (CISP), pp. 894-897, 16-18 Oct. 2010.

[21] T.W. Nattkemper, H. Wersing, W. Schubert and H. Ritter, "A neural network architecture for automatic segmentation of fluorescence micrographs", European Symposium on Artificial Neural Networks, pp. 357-367, 2000.

[22] Sjöström PJ, Frydel BR, Wahlberg LU., "Artificial Neural Network-Aided Image Analysis System for Cell Counting", Cytometry, 36:18-26 (1999).

[23] Farag, A., "Computer Based Acute Leukemia Classification", Micro-NanoMechatronics and Human Science, pp. 701-703 Vol. 2, 30-30 Dec. 2003.

[24] V. Piuri, F. Scotti, "Morphological Classification of Blood Leucocytes by Microscope Image", CIMSA 2004 – IEEE International Conference on Computational Intelligence for Measurement Systems and Applications Boston, MD, USA, 14-16 July 2004.

[25] Sheikh H, Bin Zhu, Micheli-Tzanakou, E., "Blood cell identification using neural networks.", Bioengineering Conference, pp. 119-20, 1996.

[26] F. Scotti, "Automatic Morphological Analysis for Acute Leukemia Identification in Peripheral Blood Microscope Images", IEEE International Conference on Computational Intelligence for Measurement Systems and Applications, pp. 96-101, 2005.

[27] S. S. Savkare, S. P. Narote, "Automatic Classification of Normal and Infected Blood Cells for Parasitemia Detection", IJCSNS International Jurnal of Computer Science and Network Security, Vol.11 No.2, pp. 94-97, 2011.

[28] A. M. M. et al, "Texture Based Segmentation of Cell Images using Neural Networks nad Mathematical Morphology," in IJCNN 00 – Proceedings of International Joint Conference on Neural Networks, Como, Italy, pp. 2490–2494, July 2000.

[29] L. Bertucco, G. Nunnari, C. Randieri, V. Rizza, and A. Sacco, "A cellular neural network based system for cell counting in culture of biological cells.", International Conference on Control Applications, 341– 345, Italy, Sep 1998

[30] B. Prasad, J.S. Iris Choi, and W. Badawy, "A High Throughput Screening Algorithm for Leukemia Cells", IEEE Canadian Conference on Electrical and Computer Engineering , Ottawa, pp. 2094-2097, 2006.

[31] B. Prasad, and W. Badwy, "High Throughput Algorithm for Leukemia Cell Population Statistics on a Hemocytometer", IEEE Biomedical Circuits and Systems Conference, pp. 27-30, 2007.

[32] Nasution, A.M.T., Suryaningtyas, E.K., "Comparison of Red Blood Cells Counting using two Algorithms: Connected Component Labeling and Backprojection of Artificial Neural Network", PhotonicsGlobal@Singapore, IPGC, pp. 1-4, 8-11 Dec. 2008.

[33] Mauricio, C.R.M., Schneider, F.K., Correia dos Santos, L.,"Image-Based Red Cell Counting for Wild Animal Blood", Engineering in Medicine and Biology Society (EMBS), pp. 438-441, 2010.

[34] G. P. M. Priyankara, O. W Seneviratne, R. K. O. H Silva, W. V. D Soysa and C. R. D. Silva, "An Extensible Computer Vision Application for Blood Cell Recognition and Analysis", 2006.

[35] Thomas M. Deserno, "Biomedical Image Processing", 1st ed., Springer, 2011.

[36] Anil N. Hirani, Takashi Totsuka, “Combining frequency and spatial domain information for fast interactive image noise removal”, Proceedings of the 23rd annual conference on Computer graphics and interactive techniques, p.269-276, August 1996

[37] Chen S., Shih T. Y., “On the evaluation of edge preserving smoothing filter”, Proceedings of Geoinformatics, Volume: 43, Issue: 2, 2002.

[38] Musoromy Z., Ramalingam S., Bekooy N., “Edge Detection Comparison for License Plate Detection”, Control Automation Robotics & Vision (ICARCV), pp. 1133-1138, 7-10 Dec. 2010.

[39] Canny, J. F., “A computational approach to edge detection”, IEEE Transactions. On Pattern Analysis and MachineIntelligence, 8, pp. 679-714, 1986.

[40] Marko T., Jurij F. T., “Colour spaces – perceptual, historical and applications background”, EUROCON, pp. 304-308, Slovenia, 2003.

[41] P.V.C. Hough, “Method and Means for Recognizing Complex Patterns,” U.S. Patent 3,069,654, Dec. 18 1962.

[42] Duda, R. O. and P. E. Hart, "Use of the Hough Transformation to Detect Lines and Curves in Pictures", Comm. ACM, Vol. 15, pp. 11–15 (January, 1972)

[43] T. Nattkemper, et al., “A hybrid system for cell detection in digital micrographs”, Proceedings of the IASTED International Conference on Biomedical Engineering, Innsbruck, Austria, 2004, pp. 197-200.

[44] M. Silveira, “Antibacterial activity detection and evaluation based on the detection of multiple concentric circles with the Hough transform”, Proceedings of the First Canadian Conference on Computer and Robot Vision (CRV’04), Canada, 2004, pp. 329-335.

[45] Simon Just Kjeldgaard Pedersen, Circular Hough Transform, Aalborg University , Novembre 2007.

[46] Ke-Lin Du, M.N.S. Swamy, “Neural Networks in a Softcomputing Framework“, Springer, 1st Edition, 2006.

[47] McCulloch W., Pitts W. “A logical calculus of the ideas immanent in nervous activity”, Bulletin of Mathematical Biophysics, 7:115 – 133, 1943.

[48] Rosenblatt, F. (1958). The perceptron: A probabilistic model for information storage and organization in the brain. Psychological Review, 65:386–408.

[49] Edited by S. M. Sapuan and Iqbal M. Mujtaba, “Composite Materials Technology Neural Network Applications”, CRC Press, 2010.

[50] William W. Hsieh, "Machine Learning Methods in the Environmental sciences", University of British Columbia, July 2009.

[51] S. Haykin, "Neural Networks and Learning Machines", Prentice-Hall, 3rd Ed., 2009

[52] Akın Özkan, Belgin İşgör, Hakan Tora, Pembegül Uyar, Mesude İşcan, "An Alternative Method for Cell Counting", SIU'11, IEEE Proceedings of the 19th Conference on Signal Processing and Communication Applications, Kemer, Turkey, 2011.